Supporting Information

Ward et al. 10.1073/pnas.1018875108

SI Materials and Methods

Full details of plant growth, nutrient experiments, stress treatments, feeding studies, metabolomic sample collection, NMR and DI-ESI-MS data collection, data analysis, 2D NMR, synthesis of HTGs, and 2D-NMR structural characterization are presented.

Plant Growth and Tissue Harvest. *Arabidopsis* seed was obtained from NASC, the European *Arabidopsis* Stock Center. For all experiments, *Arabidopsis* plants were grown hydroponically in a controlled environment, using the commercial Araponics system and commercial media (FloraGrow, 0.5 mL/L; FloraBloom, 1.5 mL/L; and FloraMicro, 1.0 mL/L). Seeds were germinated in seed holders filled with 0.65% agarose, and 18 seed holders were placed into a hydroponics box containing 1.9 L of nutrient medium. The hydroponics boxes (with seeds) were placed in controlled environment rooms that were set to achieve an average of 330 $\mu mol \cdot m^{-2} \cdot s^{-1}$ measured at plant growth height (~1.2 m from light source). Plants were grown under 10-h days at 23 °C day and night for the first 7 d and then under 16-h days at 21 °C from day 8 onward.

Total nutrient deprivation. At 23 d after sowing (12- to 13-leaf rosette stage), plants were moved either to a control medium (4 mM KNO_3, 0.25 mM KH_2PO_4, 0.25 mM $MgSO_4$, 0.5 mM $Ca(NO_3)_2$, 0.2 mM NaCl, and micronutrients) or to water (total nutrient depletion). Aerial tissue was harvested following 3 and 7 d of treatment. Three biological replicates were taken. Shoot and root tissue was harvested separately and directly into liquid nitrogen. The samples were lyophilized before analysis.

Comparison of stress treatments. At 24 d after sowing (12- to 13-leaf rosette stage), individual plants were selected for the stress array experiment. An array of 66, 50-mL falcon tubes was set up and a single plant was transferred to each tube, which had been prefilled with a treatment medium or the control medium. Treatments were control medium; nitrate-deplete medium; potassium-deplete medium; ammonium-based medium; osmotic stress via polyethylene glycol (PEG); salt stress; oxidative stress via hydrogen peroxide; plain water; and tubes containing control medium for root, leaf, and cold stresses. Three plants were harvested 4 d after the initial treatment and a further three plants were harvested 7 d after the initial treatment. For the cold-shock–treated plants, plants were treated 1 d before the first harvest date. Aerial and root tissue was harvested separately, directly into liquid nitrogen, and the samples were lyophilized as soon as possible after harvesting.

Stress Media Compositions.

- Control (+N) media: 4 mM KNO_3, 0.25 mM KH_2PO_4, 0.25 mM $MgSO_4$, 0.5 mM $Ca(NO_3)_2$, 0.2 mM NaCl, 14 mg/L iron chelate (sprint 330), and 1 mL/L micronutrient solution (see below).
- Nitrate-deplete media: 0.25 mM KH_2PO_4, 0.25 mM $MgSO_4$, 0.5 mM $CaCl_2$, 1.0 mM KCl, 0.2 mM NaCl, 14 mg/L iron chelate (sprint 330), and 1 mL/L micronutrient solution (see below)
- Potassium-deplete media: 4 mM $NaNO_3$, 0.25 mM NaH_2PO_4, 0.25 mM $MgSO_4$, 0.5 mM $Ca(NO_3)_2$, 0.2 mM NaCl, 14 mg/L iron chelate (sprint 330), and 1 mL/L micronutrient solution (see below)
- Ammonium-based medium: 2.5 mM $(NH_4)_2SO_4$, 0.25 mM KH_2PO_4, 0.25 mM $MgSO_4$, 0.5 mM $CaCl_2$, 0.2 mM NaCl, 1.0 mM KCl, 14 mg/L iron chelate (sprint 330), and 1 mL/L micronutrient solution (see below).
- Osmotic stress: Control media plus 10 g of PEG added to each 50-mL tube.
- Salt stress: Control media plus 0.7 g of NaCl added to each 50-mL tube.
- Oxidative stress: Control media plus 113 µL of 30% hydrogen peroxide solution (20 mM) added to each 50-mL tube.
- Water: Deionized water.
- Root damage: Control media. Roots were crushed, pinched, and rolled.
- Leaf damage: Control media. Each leaf was pinched until cut through.
- Cold treatment: Control media. The tube was placed in a −20 °C freezer for 30 min and then moved to a 4 °C refrigerator overnight.
- Micronutrients: 10 µM $MnSO_4 \cdot 4H_2O$, 24 µM H_3BO_3, 3 µM $ZnSO_4 \cdot 7H_2O$, 0.9 µM $CuSO_4 \cdot 5H_2O$, and 0.4 µM $(NH_4)_6Mo_7O_{24}$.

Resupply experiment. An array of plants was treated with the nitrate-depleted medium 26 d after sowing. Aerial tissue from individual plants was harvested 5 d after treatment, and the remaining plants were moved to control medium for 4 d before harvesting. Remaining plants were moved for a second time to the nitrate-depleted medium for 2 further days before final harvesting. Control plants were grown alongside and harvested at each harvest point.

Nitrate reductase mutants. At 23 d after sowing, Col-0 plants were moved either to a control medium (4 mM KNO_3, 0.25 mM KH_2PO_4, 0.25 mM $MgSO_4$, 0.5 mM $Ca(NO_3)_2$, 0.2 mM NaCl, and micronutrients) or to a nitrate-depleted medium [0.25 mM KH_2PO_4, 0.25 mM $MgSO_4$, 0.5 mM $CaCl_2$, 1.0 mM KCl, 0.2 mM NaCl, 14 mg/L iron chelate (sprint 330), and 1mL/L micronutrient solution]. Nitrate reductase mutants were also moved to the nitrate-deplete medium. Aerial tissue was harvested following 5 d of treatment. The samples were lyophilized before analysis.

Feeding Studies. Plants were grown in the Araponics trays in full nutrient media as above. After 20 d trays were transferred to water, nitrate-deplete medium, or fresh full nutrient medium. After 4 d of treatment four to five outer leaves from individual plants were placed together in a bunch in a microtiter plate well, with petioles dipping into solutions containing substrate (see below for amounts) in 50 µL of water and 50 µL of well make-up solvent (full media or water to match the pretreatment). Substrates used were HMBPP (0.971 µmol/well), DXP (0.714 µmol/well), and diol [3] (1.722 µmol/well). Plates were placed in controlled-environment rooms (long days) and covered with plastic lids. Wells were topped up with 100 µL water at 2-h intervals. Half of the plants were harvested at 8.5 h after treatment. The remainder of the wells were topped up with 400 µL of water and left overnight and harvested at 24 h after treatment. Tissue from individual wells was placed into preweighed Eppendorf tubes, containing a tungsten bead, and frozen in liquid nitrogen. After lyophilization samples were milled (bead beater) to a fine powder. Each sample was prepared for NMR-MS analysis, extracting with 1 mL of deuterated solvent as described below.

HTGs and diol [3] were quantified from NMR spectra using the following chemical shift regions: HTG (major), 1.7364–1.716; HTG (minor), 1.7138–1.6995; diol, 1.6919–1.6739; and data expressed as µmol/well (Table S3).

Metabolomic Sample Preparation and Data Collection. Freeze-dried tissue was milled and weighed (in triplicate) into 1.5-mL

Eppendorf tubes for metabolite extraction. For examination of total nutrient depletion and nitrate resupply, 15 mg aerial tissue was used. For the comparison of stresses, 5 mg aerial tissue and 2 mg root tissue were used for extractions. To each dry sample, D_2O-CD_3OD (80:20) containing 0.05% wt/vol TSP-d_4 (sodium salt of trimethylsilyl-d_4-propionic acid) (1.0 mL) was added. The contents of the tube were mixed thoroughly and heated at 50 °C in a water bath for 10 min. The samples were centrifuged for 5 min and 800 μL of the supernatant was then transferred to a clean Eppendorf tube and heated at 90 °C in a water bath for 2 min to ensure that any residual enzyme activity was removed. The samples were then cooled at 4 °C for 45 min before recentrifugation for 5 min; 600 μL of the supernatant was transferred to a 5-mm NMR tube and 50 μL transferred to a septum capped glass autosampler glass vial and diluted with 80:20 H_2O:CH_3OH (950 μL) for DI-ESI-MS analysis (see later, DI-ESI-MS).

^{1}H-NMR spectra were acquired under automation at a temperature of 300 K on an Avance 600 spectrometer (Bruker Biospin) operating at 600.0528 MHz, using a 5-mm SEI probe. The residual HOD signal was suppressed by presaturation and a relaxation delay of 5 s was used. Each spectrum consisted of 128 scans (256 scans used for root tissue) of 64 K data points with a spectral width of 12 ppm. Free induction decays were automatically Fourier transformed after the application of an exponential window function with a line broadening of 0.5 Hz. Phasing and baseline correction were carried out within the instrument software. ^{1}H NMR chemical shifts were referenced to the $(CH_3)_3$ signal of TSP-d_4 at δ0.00. ^{1}H-NMR spectra were automatically reduced to .csv files using AMIX (version 3.0; Bruker Biospin, http://www.bruker-biospin.com/). Spectral intensities were scaled to the TSP-d4 peak and were reduced to integrated regions or "buckets" of equal width (0.01 ppm) covering the range δ9.50–0.5. Any residual protons in HOD and CD_2HOD peaks from δ4.865–4.775 and δ3.335–3.285, respectively, were then excluded from all datasets, as were those for the d4-TSP peak (δ0.05–δ0.05).

DI-ESI-MS. A total of 100 μL of each sample was infused into the spectrometer (Esquire 3000; Bruker Daltonics) by flow injection, using an Agilent 1100 series HPLC system with degasser, quartenary pump, and autosampler. The flow rate was 100 μL/min of 20% methanol in water. Mass spectra were recorded from 1.7 to 4.2 min after the sample entered the flow. Spectra were recorded in both positive and negative ion mode on the same sample via an alternating sequence of the two ionization modes, each time recording the average of 25 scans. The spectra were recorded over an *m/z* range of 50–1,000, using the "smart tuning" function (Bruker Daltonics) with a target mass of *m/z* 300, a trap drive and stability of 100%, and a scan speed of 13,000 (*m/z*)/s. The spectra were recorded using Ion Charge Control with a maximum accumulation time of 40 ms for 20,000 (negative mode) or 50,000 (positive mode) ions. The nebulizer pressure was 20 psi and the dry gas was 6 L/min at 350 °C.

The signals resulting from the NMR internal standard (d_4-TSP), present in every sample (+ve ion, *m/z* 195, 367, 539, 711, and 883; −ve ion, *m/z* 149, 321, 493, 665, and 837), and corresponding +1 and +2 isotope peaks were removed from the acquisition spreadsheet before importing the data set into SIMCA-P 11.0 for multivariate analysis as above.

Data Analysis. Unsupervised multivariate analyses by PCA were performed using SIMCA-P 11.0 (Umetrics, http://www.umetrics.com), using mean-centered scaling. For heatmap construction and hierarchial cluster analysis (HCA), characteristic chemical shift (NMR) and *m/z* (ESI-MS) regions were selected, normalized to unit variance, and mean centered. Heatmaps and HCA diagrams were generated in Spotfire Decisionsite v9.1.2 (http://spotfire.tibco.com), using complete linkage methods with similarity based on Euclidian distance. Chemical shift ranges used for heatmap construction were as follows: (δ): alanine, 1.495–1.465; threonine, 1.335–1.325; valine, 1.065–1.035; isoleucine, 1.025–1.005; leucine, 0.975–0.965; proline, 2.045–1.955; glycine, 3.535; tryptophan, 7.745–7.715; tyrosine, 7.1995–7.175; phenylalanine, 7.435–7.395; GABA, 2.315–2.275; glutamine, 2.475–2.435; asparagine, 2.855–2.835; aspartate, 2.805–2.785; malate, 4.345–4.265; fumarate, 6.525–6.505; [1] HTG (major), 5.725–5.685; [2] HTG (minor), 5.635–5.595; sucrose, 5.415–5.405; α-glucose, 5.225–5.195; β-glucose, 4.635–4.595; fructose, 4.015–4.005; raffinose, 5.435–5.425; maltose, 5.375–5.355; galactose, 4.575–4.545; galactinol, 5.135–5.115; adenosine, 8.345–8.335; choline, 3.215–3.195; phosphocholine, 3.225; choline sulfate, 3.235; KRR, 7.865–7.805; KGR, 8.075–8.045; scopolin, 8.035–8.005; coniferyl glycoside, 7.215–7.205; 4-methylsulfinylbutylglucosinolate, 5.025–4.995; sinapoyl malate, 7.715–7.665; glucoerucin, 2.105–2.095; and 1-methoxy-O-glucobrassicin, 7.795–7.745. Direct infusion MS characteristic ions (*m/z*) were glutamate, 146; citrate, 191; kaempferol triglycoside, 739; hydroxyglucobrassicin, 463; and 8-methylsulfinyloctyl glucosinolate, 492.

Two-Dimensional NMR for Structural Characterizations. 2D NMR spectra were acquired at a temperature of 300 K on an Avance 600 spectrometer (Bruker Biospin) operating at a ^{1}H frequency of 600.0528 MHz using a 5-mm inverse (SEI) probe, using standard Bruker pulse sequences. The HTGs in the plant extract were characterized using phase-sensitive TOCSY (60-ms spinlock) and gradient-enhanced magnitude mode COSY spectra, both with 256 T1 increments of 4,096 data points over a 10-ppm sweep width (both dimensions), the residual HOD peak being suppressed by presaturation during the 2-s relaxation delay. ^{1}H-^{13}C relationships were derived from gradient heteronuclear single quantum coherence (HSQC) (phase sensitive) and gradient heteronuclear multiple bond correlation (HMBC) (magnitude mode) with a relaxation delay of 2 s, using 256 T1 increments of 2,048 data points over a 12-ppm ^{1}H and 200-ppm ^{13}C sweep width, optimized for couplings of 150 and 8 Hz, respectively. 2D spectra were recorded using between 96 and 768 scans per T1 increment. Gradient-selective 1D-NOESY spectra were recorded with 24,576 scans of 65,536 data points over a 20-ppm sweep width, using mixing times of 500 ms with a relaxation delay of 2 s.

Synthetic HTGs were characterized as above using COSY (32 scans), HSQC (32 scans, 128 T1 increments), HMBC (64 scans, 128 T1 increments), and 2D-NOESY (presaturation during the 2-s delay, 128 T1 increments of 32 scans and 400 ms mixing time).

Gas Chromatography–Mass Spectrometry (GC-MS). Lyophilized tissue (1 mg) was treated with methoxyamine hydrochloride solution in pyridine (40 μL, 20 mg·mL^{-1}) and ribitol solution in pyridine (10 μL, 0.20 mg·mL^{-1}) at 30 °C for 90 min with constant agitation (14,00 rpm). N-methyl (N-trimethylsilyl)triflouroacetamide (70 μL) containing 1% trimethylsilyl chloride was added and allowed to react at 37 °C for 30 min (1,400 rpm).

GC-MS analysis was carried out on a Pegasus III time of flight mass spectrometer (Leco) coupled to an Agilent 6890N gas chromatograph with a deactivated quartz wool packed FocusLiner (SGE) and DB-5ms capillary column [15 m × 0.18 mm inner diameter (I.D.) × 0.18 μm film thickness with a 5-m integrated guard column]. A portion (0.5 μL) of the liquid sample was injected using a splitless injection technique with an inlet temperature of 280 °C and helium carrier gas flow of 1.4 mL/min, constant flow. The purge time was 2 min and the purge flow was 20 mL/min. The oven was set to an initial temperature of 70 °C for 2 min and then ramped at 17 °C/min to 350 °C and held for 1.5 min. The GC interface and source temperatures were 310 °C and 245 °C, respectively, and electron ionization (EI+) mass spectra were acquired from 40 to 800 atomic mass units (amu) at 70 eV from 3.75 to 20 min with an acquisition rate of 20 spectra/s.

Accurate mass determination of the aglycone fragment (*m/z* 157) was done on a Micromass GCT mass spectrometer (Waters) coupled to an Agilent 6890 Series gas chromatograph and ZB5-ms (Phenomenex) caplillary column (30 m × 0.25 mm I.D. × 0.25 μm d.f.). A portion (1 μL) of the liquid sample was injected using a splitless injection technique with an inlet temperature of 250 °C and a helium carrier gas flow of 2.0 mL·min^{-1}, constant flow. The oven was set to an initial temperature of 70 °C for 2 min and then ramped at 7 °C·min^{-1} to 350 °C and held for 5 min. The GC interface and source temperatures were set to 250 °C and EI+ (electron ionization) mass spectra were acquired from 41 to 650 amu at 70 eV from 0 to 47 min with an acquisition rate of 1 spectrum/sec.

Accurate Mass Determination of *m/z* 287, 303, and 640 Obtained by DI-ESI-MS. Accurate mass determinations on ions identified in DI-ESI-MS were carried out on a Waters (http://www.waters.com) Q-TOF 1 instrument. Samples were infused directly into the mass spectrometer by flow injection, using a syringe pump at flow rates of 30 μL/min and 50 μL/min and desolvation temperatures of 180 °C and 150 °C for positive ion and negative ion analysis, respectively. The source temperature was 100 °C and the desolvation and nebulizer gas flows were 400 L/h and 25 L/h, respectively. Spectra were recorded over an *m/z* range of 100–1,700 with an acquisition rate of 2.4 s per scan. Accurate mass spectra were determined using an external mass axis calibration and internal lock (correction) mass. Mass axis calibration was done with sodium iodide (ESI$^+$) or a mixture of sugars (G_1–G_9, ESI$^-$) and endogenous sucrose, [Sucrose + K]$^+$ or [Sucrose − H]$^-$, used as a lock mass.

Nitrate Measurement. A total of 100 μL of the NMR extract described above was evaporated to dryness and resuspended in 1 mL H_2O. The concentration of NO_3-N was determined using a Skalar SAN^{PLUS} Continuous Flow Analyzer. Conversion of NO_3-N (ppm) to nitrate concentration was achieved by multiplication of the NO_3-N level by 4.26.

Synthesis of (2*E*)-4-Hydroxy-2-Methyl-2-Buten-1-yl-*O*-D-Glucopyranoside [1], (2*E*)-1-Hydroxy-2-Methyl-2-Buten-4-yl-*O*-D-Glucopyranoside [2], and (2*E*)-2-Methyl-2-Butene-1,4-diol [3].

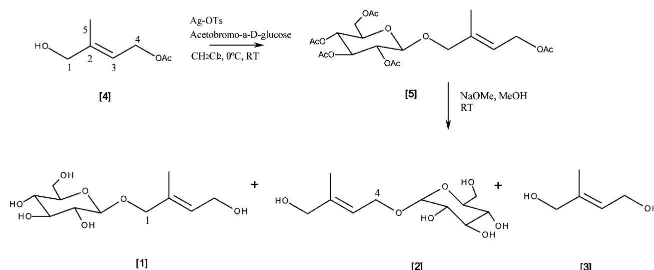

Purification of (2*E*)-Hydroxy-2-Methylbut-2-Enyl, 4-Acetate [4]. (2*E*)-Hydroxy-2-methylbut-2-enyl 4-acetate [4] was previously isolated as a synthetic intermediate in the synthesis of (2*E*)-4-hydroxy-3-methylbut-2-enyl diphosphate (HMBPP) (1). This compound was repurified, via flash chromatography, using 40:60 hexane: ethyl acetate, to give (2*E*)-Hydroxy-2-methylbut-2-enyl, 4-acetate (272 mg) as a starting material for the current synthesis.

^{1}H NMR ($CDCl_3$, 400 MHz): δ5.60 (1H, tq, J = 7 and 1.4 Hz, H-3), 4.63 (2H, d, J = 7Hz, H_2-4), 4.04 (2H, s, H_2-1), 2.05 (3H, s, OAc), and 1.72 (3H, s, H_3-5).

***O*-Glycosylation of (2*E*)-Hydroxy-2-Methylbut-2-Enyl 4-Acetate [4].** To molecular sieves (0.4 g) at 0 °C under an atmosphere of nitrogen was added silver *p*-toluenesulfonate (0.107 g). To this, a solution of (2*E*)-Hydroxy-2-methylbut-2-enyl 4-acetate ([4], 50 mg) and 2,3,4,6-Tetra-*O*-acetyl-α-D-glucopyranosyl bromide (0.214 g) in dry dichloromethane (5 mL) was added dropwise. The reaction was stirred at 0 °C for 30 min and then allowed to warm to room temperature and stirred for a further 45 min. The reaction mixture was then evaporated to yield a gray-green solid that was adsorbed onto silica gel for flash chromatography. Flash chromatography was carried out immediately using a silica gel equilibrated with 10% ethyl acetate in hexane. Increasing amounts of ethyl acetate were applied to the hexane gradient to yield, at 50% ethyl acetate, (2*E*)-4-Acetyl-2-methyl-2-butene-1,4-diol 1-(2,3,4,6-Tetra-*O*-acetyl-α-D-glucose) ([5], 10 mg).

^{1}H NMR ($CDCl_3$, 400 MHz): δ5.56 (1H, tq, J = 7 and 1.4 Hz, H-3), 4.61 (2H, d, J = 7Hz, H_2-4), 4.21 (1H, d, J = 12.7 Hz, H-1_α), 3.985 (1H, d, J = 12.7 Hz, H-1_β), 1.67 (3H, s, H_3-5), 4.48 (1H, d, J = 8 Hz, H-1′), 5.19 (1H, t, J = 9.5 Hz, H-3′), 5.08 (1H, t, J = 9.5 Hz, H-4′), 5.014 (1H, dd, J = 9.5 and 8 Hz, H-2′), 3.66 (1H, ddd, J =9.5, 4.5 and 2.5 Hz, H-5′), 4.13 (1H, dd, J = 12 and 2.5 Hz, H-6′$_\alpha$), 4.24 (1H, dd, J = 12 and 5 Hz, H-6′$_\beta$), 2.078 (3H, s, OAc), 2.05 (3H, s, OAc), -2.035 (3H, s, OAc), 2.01 (3H, s, OAc), and 1.99 (3H, s, OAc).

(2*E*)-4-Hydroxy-2-Methyl-2-Buten-1-yl-*O*-D-Glucopyranoside [1]. To a round-bottom flask containing (2*E*)-4-acetyl-2-methyl-2-butene-1,4-diol 1-(2,3,4,6-tetra-*O*-acetyl-α-D-glucose) ([5], 10 mg) under nitrogen was added a solution of sodium methoxide (0.025 M) in dry methanol. The solution was stirred at room temperature for 1.5 h. The reaction mixture was quenched with dry ice and the excess methanol evaporated in vacuo to produce a white solid (8 mg). ^{1}H 1D and 2D NMR analysis indicated a mixture (~7:2:1) of the desired (2*E*)-4-Hydroxy-2-methyl-2-buten-1-yl-*O*-D-glucopyranoside [1], the alternative (2*E*)-1-Hydroxy-2-methyl-2-buten-4-yl-*O*-D-glucopyranoside [2], and (2*E*)-2-Methyl-2-butene-1,4-diol [3].

(2*E*)-4-Hydroxy-2-Methyl-2-Buten-1-yl-*O*-D-Glucopyranoside [1].

^{1}H NMR (CD_3OD, 400 MHz): δ5.67 (1H, br. t, H-3), 4.27 (1H, d, J = 8 Hz, H-1′), 4.23 (1H, d, J = 12 Hz, H-1_β), 4.13 (2H, d, J = 7 Hz, H_2-4), 4.07 (1H, d, J = 12Hz, H-1_α), 3.86 (1H, dd, J = 12 and 2 Hz, H-6′), 3.66 (1H, dd, J = 12 and 5.5 Hz, H-6′), 3.19–3.28 (4 × 1H, m, H-2′, H-3′, H-4′, H-5′), and 1.72 (3H, s, H_3-5).

^{1}H NMR (D_2O:CD_3OD 8:2, 400 MHz): δ5.69 (1H, br. t, H-3), 4.42 (1H, d, J = 8 Hz, H-1′), 4.27 (1H, d, J = 12 Hz, H-1_β), 4.17 (2H, d, J = 7 Hz, H_2-4), 4.15 (1H, d, J = 12 Hz, H-1_β), 3.89 (1H, dd, J = 12 and 2 Hz, H-6′), 3.70 (1H, dd, J = 12 and 5 Hz, H-6′), and 1.72 (3H, s, H_3-5).

^{1}H NMR (CD_3OD, 600 MHz): δ5.67 (1H, tq, J = 7 and 1.4 Hz, H-3), 4.27 (1H, d, J = 8 Hz, H-1′), 4.23 (1H, d, J = 12 Hz, H-1_β), 4.13 (2H, d, J = 7 Hz, H_2-4), 4.07 (1H, d, J = 12 Hz, H-1_α), 3.85 (1H, dd, J = 12 and 2 Hz, H-6′), 3.66 (1H, dd, J = 12 and 5.5 Hz, H-6′), 3.19–3.28 (4 × 1H, m, H-2′, H-3′, H-4′, H-5′), and 1.72 (3H, s, H_3-5).

^{1}H NMR (D_2O:CD_3OD 8:2, 600 MHz): δ5.69 (1H, tq, J = 7 and 1.4 Hz, H-3), 4.42 (1H, d, J = 8 Hz, H-1′), 4.27 (1H, d, J = 12 Hz, H-1_β), 4.18 (2H, d, J = 7 Hz, H_2-4), 4.15 (1H, d, J = 12 Hz, H-1_β), 3.89 (1H, dd, J = 12 and 2 Hz, H-6′), 3.70 (1H, dd, J = 12 and 5 Hz, H-6′), and 1.725 (3H, s, H_3-5).

^{13}C NMR (CD_3OD, 600 MHz): δ135.7 (C-2), 128.1 (C-3), 102.1 (C-1′), 75.2 (C-1), 62.8 (C-6′), 59.1 (C-4), 14.3 (C-5), 62.75 (C-6′), 75.2 (C-5′/C-3′), 77.95 (C-3′/C-5′), and 71.65 (C-2′/C-4′).

(2*E*)-1-Hydroxy-2-Methyl-2-Buten-4-yl-*O*-D-Glucopyranoside [2].

^{1}H NMR (CD_3OD, 400 MHz): δ5.63 (1H, br. t, H-3), 4.29 (1H, d, J = 8 Hz, H-1′), 4.36–4.2 (2 × 1H, H_2-4), 3.96

(2H, br. s, H_2-1), 3.83–3.66 (2 × 1H, m, H_2-6′), 3.17–3.28 (4 × 1H, m, H-2′, H-3′, H-4′, H-5′), and 1.70 (3H, s, H_3-5).

^{1}H NMR (CD_3OD, 600 MHz): δ5.63 (1H, tq, J = 7 and 1.4 Hz, H-3), 4.29 (1H, d, J = 8 Hz, H-1′), 4.36–4.2 (2 × 1H, H_2-4), 3.96 (2H, br. s, H_2-1), 3.83–3.66 (2 × 1H, m, H_2-6′), 3.17–3.28 (4 × 1H, m, H-2′, H-3′, H-4′, H-5′), and 1.70 (3H, s, H_3-5).

^{1}H NMR (D_2O:CD_3OD 8:2, 600 MHz): δ5.60 (1H, tq, J = 7 and 1.4 Hz, H-3), 4.02 (2H, br. s, H_2-1), 3.83–3.66 (2 × 1H, m, H_2-6′), 3.17–3.28 (4 × 1H, m, H-2′, H-3′, H-4′, H-5′), and 1.70 (3H, s, H_3-5).

^{13}C NMR (CD_3OD, 600 MHz): δ140.6 (C-2), 121.6 (C-3), 104.3 (C-1′), 68.0 (C-1), 66.1 (C-4), and 13.8 (C-5).

(2E)-2-Methyl-2-Butene-1,4-Diol [3].

^{1}H NMR (CD_3OD, 400 MHz): δ5.59 (1H, br. t, H-3), 4.13 (2H, d, 6.3Hz, H_2-4), 3.94 (2H, s, H_2-1), and 1.67 (3H, s, H_3-5).

^{1}H NMR (D_2O:CD_3OD 8:2, 400 MHz): δ5.59 (1H, br. t, H-3), 4.17 (2H, d, 6.3Hz, H_2-4), 3.999 (2H, s, H_2-1), and 1.68 (3H, s, H_3-5).

^{1}H NMR (D_2O:CD_3OD 8:2, 600 MHz): δ5.59 (1H, tq, J = 7 and 1.4 Hz, H-3), 4.17 (2H, d, 7 Hz, H_2-4), 3.998 (2H, s, H_2-1), and 1.68 (3H, s, H_3-5).

^{1}H NMR (CD_3OD, 600 MHz): δ5.59 (1H, tq, J = 7 and 1.4 Hz, H-3), 4.13 (2H, d, J = 7 Hz, H_2-4), 3.94 (2H, s, H_2-1), and 1.67 (3H, s, H_3-5).

^{13}C NMR (CD_3OD, 600 MHz): δ138.8 (C-2), 124.7 (C-3), 68.4 (C-1), 59.1 (C-4), and 14.0 (C-5).

Two-Dimensional NMR Studies (CD_3OD) on Synthetic (*2E*)-4-Hydroxy-2-Methyl-2-Buten-1-yl-*O*-D-Glucopyranoside [1].

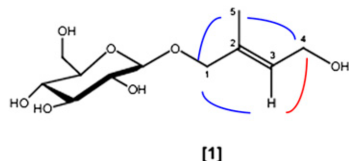

[1]

COSY correlations (red) were observed between 3-H and 4-H_2.

NOESY correlations (blue) were observed between 5-H_3 and 4-H_2, 3-H and 1-H_2, and 5-H_3 and 1-H_2. This result indicated a *trans* configuration as no NOESY correlation was observed between 1-H_2 and 4-H_2 or between 3-H and 5-H_3.

HSQC revealed information on ^{1}H and ^{13}C chemical shifts for each part of the molecule:

5-H_3 (br s, δ1.72) correlated with 5-C (δ14.3).
3-H (m, δ5.67) correlated with 3-C (δ128.1).
1-H_α (d, J = 12 Hz, δ4.07) correlated with 1-C (δ75.2).
1-H_β (d, J = 12 Hz, δ4.23) correlated with 1-C (δ75.2).
4-H_2 (d, J = 7 Hz, 4.13) correlated with 4-C (δ59.1).
1′-H (d, J = 8 Hz, δ4.27) correlated with 1′-C (δ102.1).

HMBC revealed information on ^{1}H and ^{13}C connectivities and confirmed the position (C-1) of glycosylation: (key correlations are underlined).

1′-C (δ102.1) correlated with 1-H_α (d, J = 12 Hz, δ4.07) and 1-H_β (d, J = 12 Hz, δ4.23).
5-C (δ14.3) correlated with 3-H (m, δ5.67), 1-H_α (d, J = 12 Hz, δ4.07), and 1-H_β (d, J = 12 Hz, δ4.23).
4-C (δ59.1) correlated with 1-H_α (d, J = 12 Hz, δ4.07) and 1-H_β (d, J = 12 Hz, δ4.23).
3-C (δ128.1) correlated with 1-H_α (d, J = 12 Hz, δ4.07), 1-H_β (d, J = 12 Hz, δ4.23), 4-H_2 (d, J = 7 Hz, 4.13), and 5-H_3 (br s, δ1.72).
2-C (δ135.7) correlated with 1-H_α (d, J = 12 Hz, δ4.07), 1-H_β (d, J = 12 Hz, δ4.23), 4-H_2 (d, J = 7 Hz, 4.13), and 5-H_3 (br s, δ1.72).
1-C (δ75.2) correlated with 3-H (m, δ5.67), 1′-H (d, J = 8 Hz, δ4.27), and 5-H_3 (br s, δ1.72).

Note that no HMBC correlation was observed between 1′-C and 4-H_2 or between 4-C and 1′-H_2.

2D correlations on the 4-glycoside [2] were more difficult to elucidate fully, due to the lower concentration of this metabolite in the synthetic mixture. Despite this, HMBC correlations could be observed between 4-H_2 (δ4.36–4.20) and 2-C (δ140.6), 3-C (δ121.6), and 1′-C (δ 102.95), confirming the site of glycosylation in the minor synthetic product.

1. Ward JL, Beale MH (2002) Synthesis of (2*E*)-4-hydroxy -3-methylbut-2-enyl diphosphate, a key intermediate in the biosynthesis of isoprenoids. *J Chem Soc Perkin Trans 1* 6:710–712.

Fig. S1. The terpenoid pathway in plastids and its relationships with the PP pathway and CO_2 and N assimilation. Abbreviations: E4P, erythrose-4-phosphate; FPP, farnesyl diphosphate; G-3-P, glycerate 3-phosphate; RuBP, ribulose 1,5-bis phosphate; GAP, glyceraldehyde-3-phosphate; PEP, phosphoenolpyruvate; *PEPC*, phosphoenolpyruvate carboxylase; DXP, deoxyxylulose 5-phosphate; *DXS*, deoxyxylulose phosphate synthase; MEP, methylerythritol 4-phosphate; MEcPP, methylerythritol 2,4-cyclodiphosphate; *HDS*, 4-hydroxymethylbut-2-enyl diphosphate synthase; *HDR*, 4-hydroxymethylbut-2-enyl diphosphate reductase; *IS*, isoprene synthase.

Fig. S2. 2D-NMR analysis of spectra from nutrient-deprived *Arabidopsis* leaves. (*A*) 1D selective NOESY spectra. Irradiation of H-3 gives enhancement of H-1α and H-1β and H_2-4 signals whereas irradiation of H_3-5 gives enhancement of H_2-4 signals. Spectra are phased such that irradiated signals are positive and enhancements are negative. (*B*) 2D-COSY spectra and projections. (*C*) Significant correlations obtained from 2D experiments: (*C*, *i*) NOESY correlations from 1D selective NOESY; (*C*, *ii*) COSY correlations; and (*C*, *iii*) HMBC correlations indicating long-range coupled ^1H and ^{13}C.

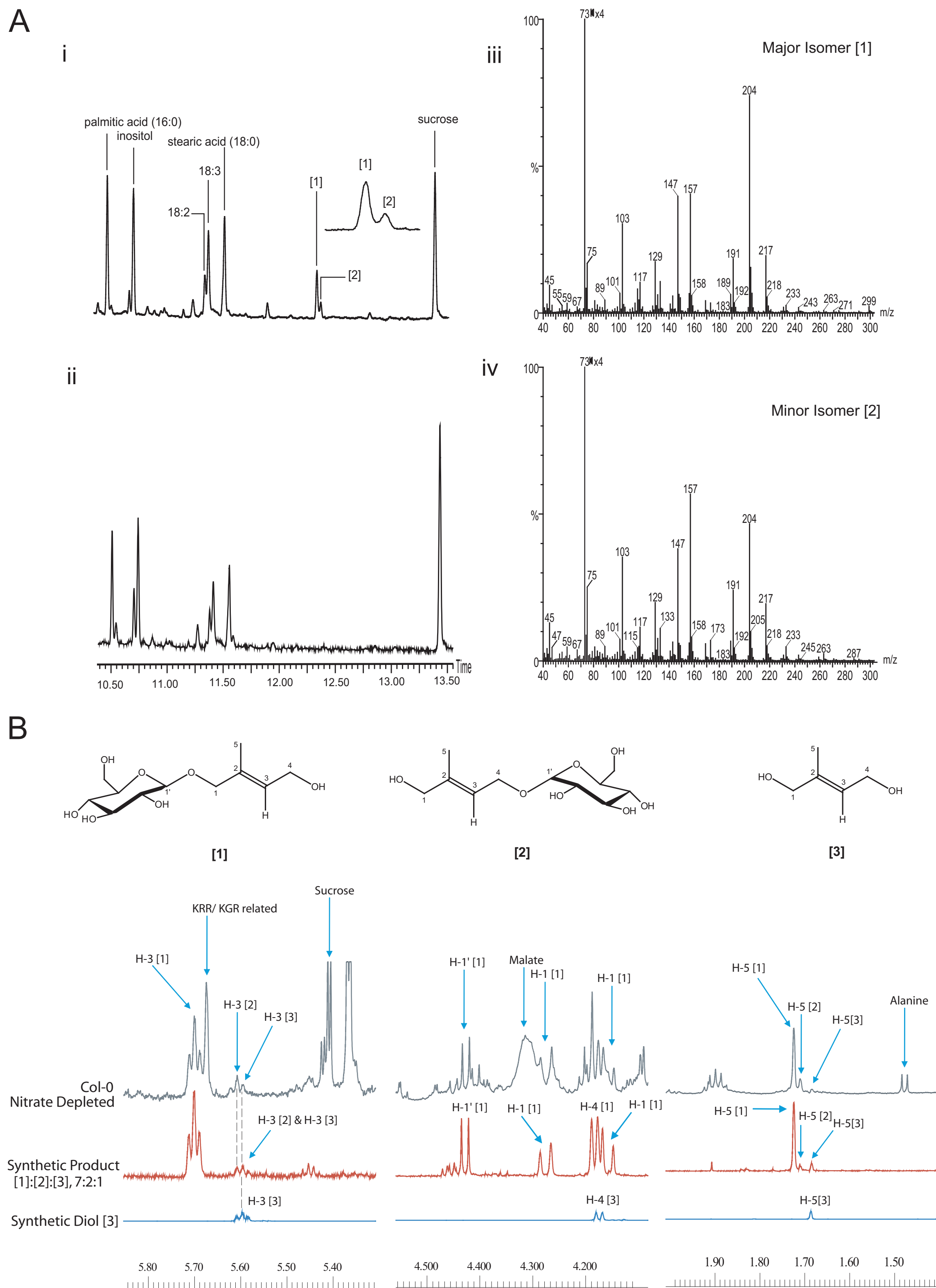

Fig. S3. (*A*) GC-MS analysis of nutrient-deprived *Arabidopsis* (7 d). (*A*, *i*) Total ion chromatogram of nutrient-deprived leaf tissue; (*A*, *ii*) total ion chromatogram of control; (*A*, *iii*) mass spectrum of major HTG isomer [1]; and (*A*, *iv*) mass spectrum of minor HTG isomer [2]. (*B*) Comparison of sections of ^{1}H-NMR data of synthetic HTGs (red) with those obtained in nitrate-depleted Col-0 extract (black) and synthetic diol [3] (blue).

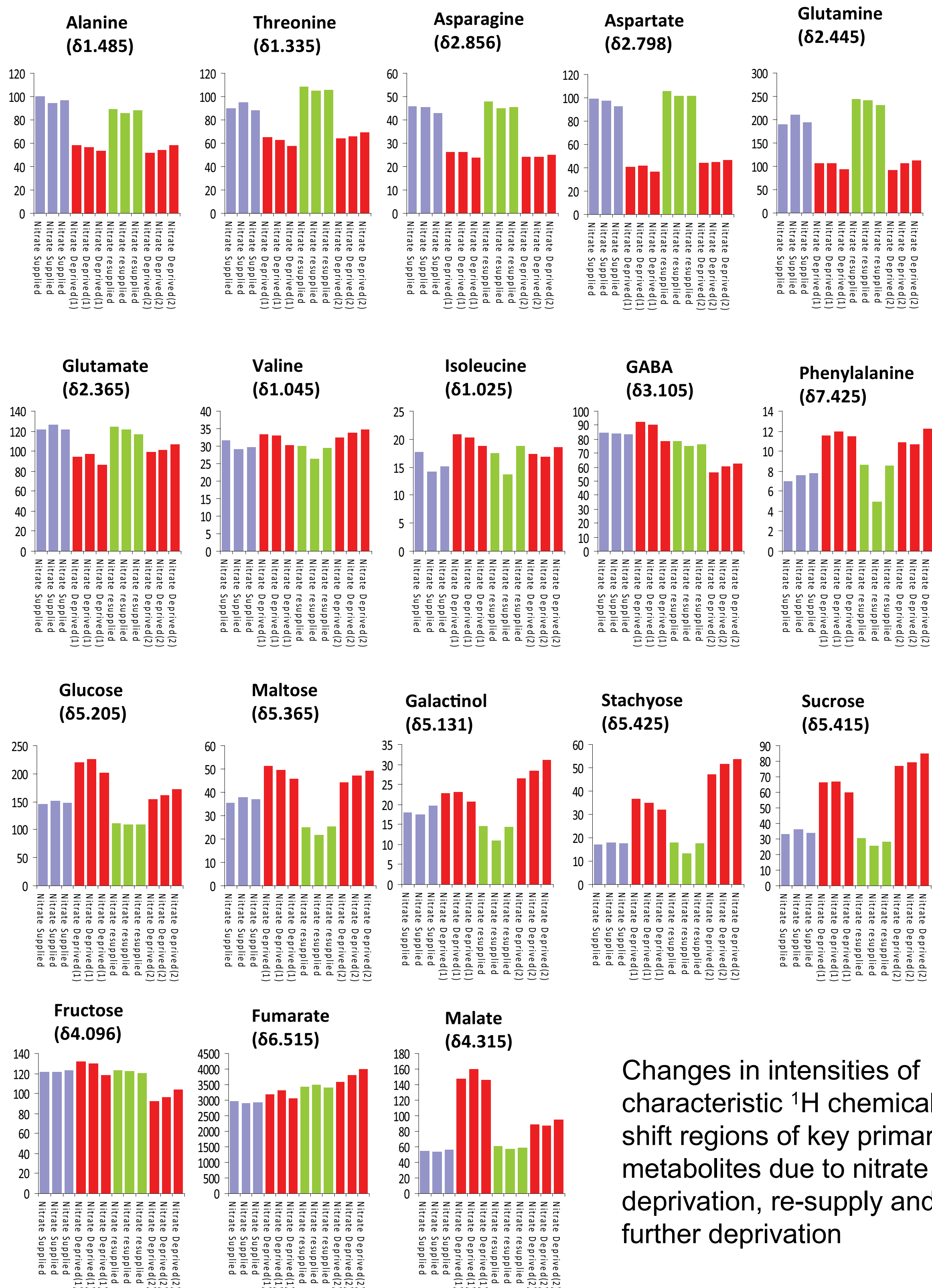

Fig. S4. Changes in intensities of characteristic chemical shifts for key metabolites (leaf tissue) due to nitrate deprivation and resupply.

Fig. S5. Section of negative ion mode DI-ESI-MS data from (*A*) nitrate-supplied and (*B*) nitrate-deprived Col-0 samples indicating a flavonoid–nitrate adduct (*m/z* 640) in nutrient-supplied samples and its absence in nitrate-limited samples.

Fig. S6. Comparison of ^{1}H-NMR spectra (δ8.50–4.50) from nitrate-supplied roots and nitrate-deprived roots with those from authentic standard compounds run under the same conditions. S, scopolin; CG, coniferyl glycoside.

Table S1. Comparison of ^{1}H and ^{13}C NMR chemical shift regions for synthetic and previously reported hemiterpene glycosides [1] and [2] and the diol [3]

	Synthetic *E*-1-O-Glyc [1] (CD_3OD), 400 MHz	Literature value of *E*-1-O-Glyc(CD_3OD) (1)	Synthetic *E*-4-O-Glyc [2] (CD_3OD), 400 MHz	Literature value of *E*-4-O-Glyc (CD_3OD) (2)	Synthetic *E*-1,4-diol [3], (CD_3OD), 400 MHz	Literature value of *E*-1,4-diol (CD_3OD) (1)
^{1}H assignments						
1-H_α	4.07 (d, 12)	3.97 (d, 12.4)	3.96 (br. S)	3.96 (s)	3.999 (s)	3.93 (br. S)
1-H_β	4.23 (d, 12)	4.13 (d, 12.4)				
3-H	5.67 (br. t)	5.61 (t, 6.8)	5.63 (br. t)	5.63 (t, 6.8)*	5.59 (br. t)	5.59 (br. t)
4-H_α	4.13 (d, 7)	4.06 (d, 6.8)	4.36–4.20 (2 × 1H m)	4.39 (dd, 12.1, 6.2)	4.17 (d, 6.3)	4.13 (d)
4-H_β				4.28 (m)		
5-H_3	1.72 (br s)	1.61 (s)	1.70 (s)	1.69 (s)	1.68 (s)	1.67 (s)
1′-H	4.27 (d, 8)	4.24 (d, 7.8)	4.29 (d, 8)	4.29 (d, 8)		
2′-H	3.19–3.28 (m)	3.19–3.28	3.17–3.28 (m)	3.17 (m)		
3′-H				3.34 (m)		
4′-H				3.25 (m)		
5′-H				3.31 (m)		
6′-H_α	3.66 (dd, 12, 5.5)	Not reported	3.83–3.66 (m)	3.67 (dd, 11.7, 4.9)		
6′-H_β	3.83 (dd, 12, 2)	Not reported		3.87 (br d, 11.7)		
^{13}C assignments						
1-C	75.2	74.5	68.1	68.0	68.4	68.2
2-C	135.7	134.4	140.6	140.9	138.8	138.7
3-C	128.1	127.1	121.6	121.7	124.7	125.0
4-C	59.1	58.5	66.4	66.2	59.1	59.2
5-C	14.3	13.9	13.87	13.9	14.1	13.7
1′-C	102.1	101.9	102.95	103.0		
2′-C	75.0	73.9	n.d.	75.1		
3′-C	78.1 or 77.9	76.3 or 76.8	n.d.	78.2		
4′-C	71.53	70.5	n.d.	71.7		
5′-C	78.1 or 77.9	76.8 or 76.3	n.d.	78.1		
6′-C	62.8	61.9	n.d.	62.8		

*Corrected literature value from personal communication with R. Nishida, corresponding author of ref. 2. All chemical shifts are relative to internal trimethylsilane (TMS).

1. Nicoletti M, Tomassini L, Foddai S (1992) A new hemiterpenoid glucoside from *Ornithogalum montanum*. *Planta Med* 58:472.
2. Ohta N, Mori N, Kuwahara Y, Nishida R (2006) A hemiterpene glucoside as a probing deterrent of the bean aphid, *Megoura crassicauda,* from a non-host vetch, *Vicia hirsuta*. *Phytochemistry* 67:584–588.

Table S2. Concentrations of hemiterpene glycosides observed from substrate feeding to nutrient-starved plants

Code pretreatment-substrate-timepoint	Amount of substrate added, μmol/well	HTG major, μmol/well	HTG minor, μmol/well	Diol, μmol/well	Total HTG, μmol/well	Total HTG plus diol, μmol/well	% conversion
Control-none-1	—	—	—	—	—	—	
Ndeplete-none-1	—	0.0154 ± 0.0030	0.0059 ± 0.0003	0.0041 ± 0.0004	0.0213 ± 0.0027	0.0254 ± 0.0023	—
Water-none-1	—	0.0307 ± 0.0024	0.0117 ± 0.0004	0.0068 ± 0.0010	0.0424 ± 0.0027	0.0492 ± 0.0017	—
Control-none-2	—	—	—	—	—	—	—
Ndeplete-none-2	—	0.0190 ± 0.0087	0.0073 ± 0.0012	0.0018 ± 0.0017	0.0262 ± 0.0099	0.0280 ± 0.0116	—
Water-none-2	—	0.0542 ± 0.0024	0.0206 ± 0	0.0018 ± 0.0015	0.0874 ± 0.0025	0.0892 ± 0.0010	—
Control-HMBPP-1	0.971	0.0921 ± 0.0238	0.0361 ± 0.0028	0.0415 ± 0.0033	0.1282 ± 0.0267	0.1697 ± 0.0233	17.5
Ndeplete-HMBPP-1	0.971	0.1014 ± 0.0150	0.0378 ± 0.0012	0.0746 ± 0.0071	0.1392 ± 0.0162	0.2137 ± 0.0233	22.0
Water-HMBPP-1	0.971	0.1649 ± 0.0263	0.0602 ± 0.0030	0.0861 ± 0.0238	0.2251 ± 0.0251	0.3112 ± 0.0013	32.0
Control-HMBPP-2	0.971	0.2178 ± 0.0165	0.0801 ± 0.0062	0.0118 ± 0	0.2979 ± 0.0227	0.3097 ± 0.0227	31.9
Ndeplete-HMBPP-2	0.971	0.1809 ± 0.0472	0.0706 ± 0.0013	0.0040 ± 0.0049	0.2515 ± 0.0485	0.2555 ± 0.0534	26.3
Water-HMBPP-2	0.971	0.3070 ± 0.0251	0.1170 ± 0.0004	0.0015 ± 0.0006	0.4240 ± 0.0254	0.4255 ± 0.0248	43.8
Control-diol-1	1.722	0.2557 ± 0.0320	0.0993 ± 0.0129	0.6349 ± 0.0372	0.3550 ± 0.0448	0.9900 ± 0.0077	57.5
Ndeplete-diol-1	1.722	0.1464 ± 0.0076	0.0338 ± 0.0055	0.4853 ± 0.0778	0.1802 ± 0.0130	0.6654 ± 0.0908	38.6
Water-diol-1	1.722	0.3306 ± 0.0320	0.1262 ± 0.0008	0.4774 ± 0.0433	0.4562 ± 0.0328	0.9342 ± 0.0761	54.2
Control-diol-2	1.722	0.7130 ± 0.0057	0.2547 ± 0.0258	0.0123 ± 0.0050	0.9678 ± 0.0315	0.9801 ± 0.0265	56.9
Ndeplete-diol-2	1.722	0.5702 ± 0.2463	0.1276 ± 0.0004	0.1452 ± 0.1922	0.6978 ± 0.2459	0.8430 ± 0.0537	48.9
Water-diol-2	1.722	0.8156 ± 0.0730	0.2041 ± 0.0187	0.0110 ± 0.0042	1.0198 ± 0.0543	1.0308 ± 0.0585	59.8
Control-DXP-1	0.714	0.0377 ± 0.0081	0.0068 ± 0.0022	0.0055 ± 0.0005	0.0445 ± 0.0104	0.0500 ± 0.0109	7.0
Ndeplete-DXP-1	0.714	0.0476 ± 0.0038	0.0182 ± 0.0010	0.0519 ± 0.0014	0.0658 ± 0.0047	0.1177 ± 0.0061	16.5
Water-DXP-1	0.714	0.1201 ± 0.0067	0.0182 ± 0.0086	0.0158 ± 0.0013	0.1383 ± 0.0153	0.1541 ± 0.0166	21.6
Control-DXP-2	0.714	0.0480 ± 0.0023	0.0054 ± 0.0057	0.0040 ± 0.0005	0.0534 ± 0.0034	0.0573 ± 0.0029	8.0
Ndeplete-DXP-2	0.714	0.1246 ± 0.0176	0.0329 ± 0.0093	0.0147 ± 0.0023	0.1575 ± 0.0270	0.1722 ± 0.0293	24.1
Water-DXP-2	0.714	0.2208 ± 0.0495	0.0467 ± 0.0134	0.0337 ± 0.0144	0.2676 ± 0.0629	0.3012 ± 0.0773	42.1